ELSEVIER

Solar Energy Materials & Solar Cells 72 (2002) 465–472

Solar Energy Materials & Solar Cells

www.elsevier.com/locate/solmat

Room-temperature luminescence and electron-beam-induced current (EBIC) recombination behaviour of crystal defects in multicrystalline silicon

M. Kittler[a,*,1], W. Seifert[1,a], T. Arguirov[1,b], I. Tarasov[c], S. Ostapenko[c]

[a] *IHP, Im Technologiepark 25, 15236 Frankfurt (Oder), Germany*
[b] *BTU Cottbus, Erich-Weinert-Strasse 1, 03044 Cottbus, Germany*
[c] *University of South Florida, Tampa, FL 33620, USA*

Abstract

Crystal defects such as dislocations and grain boundaries may show a detrimental influence on solar cell performance due to their recombination activity. The contamination of the defects by impurities strongly affects their recombination strength. Recently, it was shown that the temperature behaviour of the recombination activity of defects measured with EBIC, $c(T)$, gives a quantitative access to the amount of contamination at dislocations. We have compared the mapping of the band-to-band and the defect (D1) photoluminescence (PL), measured at room temperature in multicrystalline Si, with the electron-beam-induced current temperature behaviour. Intensive D1 luminescence band and a remarkable reduction of the band-to-band PL intensity are observed at the defect sites. We have found that wafer regions with pronounced D1 band corresponds to dislocations with a weak contamination level down to a few tens of impurity atoms per μm of the dislocation length.

Keywords: Photoluminescence; D-bands; Band-band luminescence; SiPHER®; EBIC; Recombination behaviour; Crystal defects

*Corresponding author. Tel.: +49-335-5625-130; fax: +49-335-5625-327.
E-mail address: kittler@ihp-microelectronics.com (M. Kittler).
[1] Joint Lab IHP/BTU.

0927-0248/02/$ - see front matter
PII: S0927-0248(01)00194-5

1. Introduction

It is known that dislocations in multicrystalline silicon (mc-Si) cause a decrease in the minority-carrier lifetime or diffusion length, respectively. Thus, the defects may essentially reduce the solar cell efficiency [1]. The temperature behaviour of the defect contrast, $c(T)$, as measured by the technique of the electron-beam-induced current (EBIC), allows to quantitatively characterise the dislocation recombination activity. The $c(T)$ recombination behaviour of dislocations was found to be mainly affected by metal impurity contamination [2]. Different types of $c(T)$ behaviour can be distinguished, as shown in Fig. 1. Clean dislocations show a very small activity only, with a maximum of the contrast at about 50–70 K (type II). Small contamination levels enhance the activity at low temperatures while the room-temperature activity remains negligible (type 2). Room-temperature activity appears at higher contamination levels, resulting first in the mixed type behaviour with dislocations still having its largest activity at low temperatures. With further enhancement of the contamination, a qualitative change in the dislocation behaviour is observed: the activity increases with rising temperature (type 1). Further increase of the contamination level, which leads to a decoration of the dislocations with metal silicide precipitates, causes a rise in the activity to a very high level (type I). The observations on the $c(T)$ behaviour—except the type I in Fig. 1, which is due to the metal silicide precipitates acting as internal Schottky barriers [3]—can be understood by a new model [4]. The model assumes that shallow one-dimensional dislocation bands, induced by the dislocation strain field, and deep electronic levels, caused by segregated impurity atoms at the dislocations, can exchange electrons and holes. As a consequence, the recombination of carriers captured at the dislocation bands can be drastically enhanced by the presence of even small concentrations of impurity

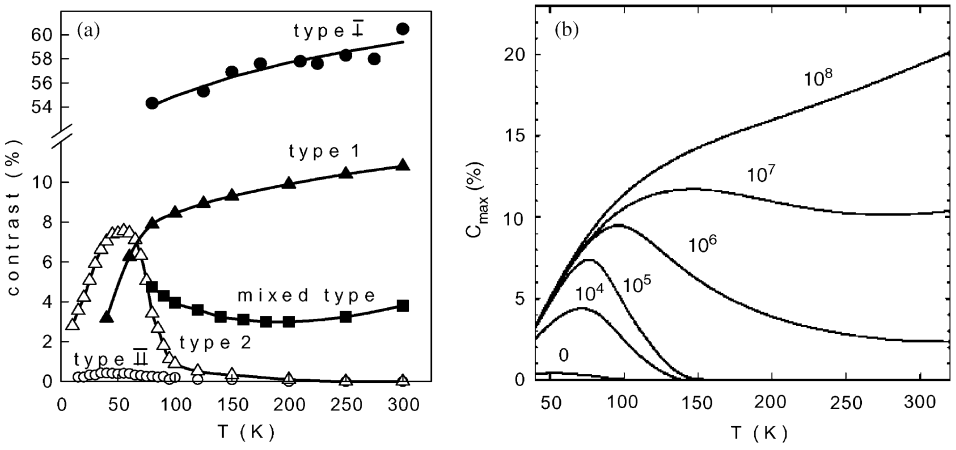

Fig. 1. Temperature dependence of EBIC contrast, $c(T)$, of dilsocations for different contamination levels: (a) experimental results, change of the contrast type in the following sequence with increasing contamination level: II→2→mixed→1→I; (b) contrast simulation [4], parameter is the line density N_M of deep levels decoarting the dislocation (in cm^{-1}).

atoms at the dislocation core. Fig. 1 compares the experimental $c(T)$ data with simulated curves. It clearly demonstrates that even a small contamination with deep metal impurities of only 1 impurity atom/μm of the dislocation length, for instance, leads to a strong increase in the recombination as compared to clean dislocations. The model allows to estimate the concentration of the deep-level impurities at dislocations from the experimental $c(T)$ data.

Besides the electrical activity, dislocations exhibit very intriguing optical properties. Already, more than 20 years ago, the characteristic D-band lines associated with dislocations were observed in the photoluminescence (PL) spectra of Si [5–7]. Among them, the quartet of D1–D4 lines represents the main dislocation feature. Generally, the D-lines were found to occur in luminescence spectra taken at low temperatures between 4.2 and 77 K in high-purity Cz or FZ silicon. At room temperature, only the D1-line of the dislocation quartet persists. This is illustrated in Fig. 2 [8–10]. The state of understanding regarding the nature of the different D-lines can be summarised as follows: D4 (1.0 eV) is related to the transition between the shallow one-dimensional dislocation bands and D3 (0.96 eV) is its phonon replica [10]. The nature of the lines D1 (0.8 eV) and D2 (0.87 eV) is still controversial. However, they are often related to kinks, jogs and stacking faults in the vicinity of dislocations [11]. Different suggestions on the nature of D1 and D2 and the energy levels involved can be found, for instance, in Refs. [12,10]. Furthermore, it was observed that the appearance of the D-bands depends on the concentration of point defects and their clusters contaminated a dislocation. Higgs et al. [2,13,14] demonstrated that D-band emission in low-temperature PL and cathodoluminescence appears at dislocations with types 1, 2, and mixed-type EBIC behaviour. D-band luminescence was not detected for dislocations of types I and II, however. That means that D-band luminescence seems to originate only from dislocations with a moderate level of

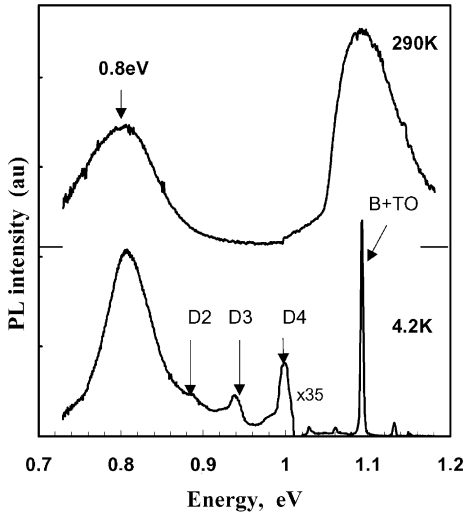

Fig. 2. Photoluminescene spectra at 4.2 and 290 K in EFG Si foils at a location with strong D1 (0.8 eV) luminescence. Excitation with a 800 nm IR laser at 100 mW/cm^2 [8].

contamination. If the contamination level is too low (type II behaviour of clean dislocations) or too high (decoration with metal silicide precipitates, type I behaviour), D-band luminescence vanishes. An explanation as to why the dislocation should be moderately decorated to cause the D-bands is still lacking.

Both the band-to-band luminescence and the defect (D1) luminescence can be utilised for the purpose of non-contact characterisation of Si at room temperature. For high-resolution mapping of defects, a dedicated PL system called Si Photo Enhanced Recombination (SiPHER®) has been developed and is commercially available [15]. The system uses the room-temperature band-to-band luminescence, which is the highest in perfect Si material and decreases at the defect sites because of competitive electron–hole recombination through the defect states. Independently, recording the D1-band luminescence provides another opportunity to study crystal defects/dislocations by room-temperature PL [8,9].

In this paper, we present a comparison of defect imaging by room-temperature PL and EBIC. EBIC serves as a tool to (i) identify the defects and (ii) estimate their level of contamination by impurities. The estimate of the contamination level is based on the temperature behaviour of the EBIC defect contrast, $c(T)$. We will show that a low contamination level is sufficient to image defects with both band-to-band and D1 luminescence.

2. Results

2.1. Sample 1

An mc-Si sample prepared by block casting was investigated at room temperature by EBIC and the SiPHER® technique. To ensure SiPHER analysis, the sample was chemo-mechanically polished before the investigation. Two micrographs comparing the same sample area are given in Fig. 3. The bright regions in the EBIC micrograph

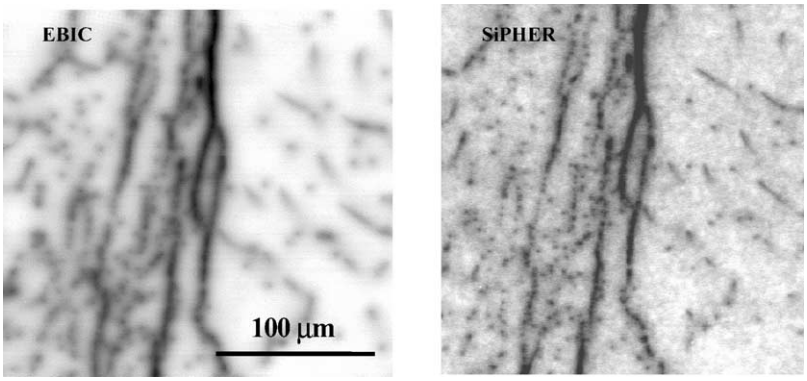

Fig. 3. Comparison of EBIC (30 keV) and band-to-band luminescence/SiPHER (532 nm) on block-cast mc-Si.

correspond to places without crystal defects, where the diffusion length is relatively high ($>100\,\mu m$). The dark contrasts are due to recombination-active crystal defects such as dislocations and grain boundaries. The appearance of EBIC contrast at room-temperature points to a rather high contamination of the defects/dislocations. The contamination level can be roughly estimated to be a few 100–1000 metal atoms/μm dislocation length (compare also Fig. 1). This relatively high defect contamination is probably caused by the applied polishing procedure [16,17]. The SiPHER image displays the intensity of the band-to-band emission, where the bright and dark areas characterise regions with high and low luminescence intensity, respectively. It can be seen that the defect pattern on both the micrographs is practically identical, demonstrating that both methods reveal the same defects. The spatial resolution of both methods appears to be comparable. Regarding the sensitivity of SiPHER, we can state that the technique allows to detect defects with a rather strong contamination. From a previous comparison with oxygen-related defects in Si, however, we expect that defects with a lower contamination level (appearing in EBIC only at temperatures below 300 K, i.e. type 2 behaviour) can be detected with SiPHER, too.

2.2. Sample 2

EFG Si foils have been examined by PL and EBIC. An apparatus was designed to study PL at room temperature for both, the band–band and D1 band emission. Experimental details of spectroscopic room-temperature PL mapping system can be found in Ref. [9]. The mapping system allows scanning the sample for defects without sophisticated preliminary preparation, but at lower spatial resolution in comparison to the EBIC technique. A typical room-temperature PL spectrum measured in the area of high recombination activity at 4.2 K and room temperature is shown in Fig. 2. It was previously revealed that the mapping contrast of the band-to-band PL intensity and the "defect" PL intensity are essentially reversed: high "defect" band intensity corresponds to low and opposite band-to-band PL.

Fig. 4 compares micrographs of room-temperature PL with EBIC. The PL images display the intensity of band-to-band (Fig. 4a) and D1 (Fig. 4b) luminescence across the sample. The corresponding EBIC micrographs taken at 300 and 80 K are shown in Figs. 4c and d, respectively. Altogether, a good correlation between the micrographs is found. The regions of low band-to-band and high D1 luminescence are identified as having been caused by dislocations. Some obvious differences are due to the much higher spatial resolution of EBIC as compared to the PL maps. The D1 luminescence appears complementary to the band-to-band one and arises at the defect sites, which are seen in EBIC both at 300 and 80 K. It is important to note that the EBIC contrast is strongly reduced at room temperature, indicating type 2 behaviour (see Fig. 1a). Fig. 5 depicts profiles of the EBIC collection efficiency taken at 300 and 80 K, respectively, along the scanning line marked in Fig. 4. The defect-rich regions consisting of densely packed dislocations show a low collection efficiency at 80 K. This corresponds to a strong recombination activity at this temperature. At room temperature, the recombination activity of the defects is much weaker since the reduction of the collection efficiency at the dislocations was found

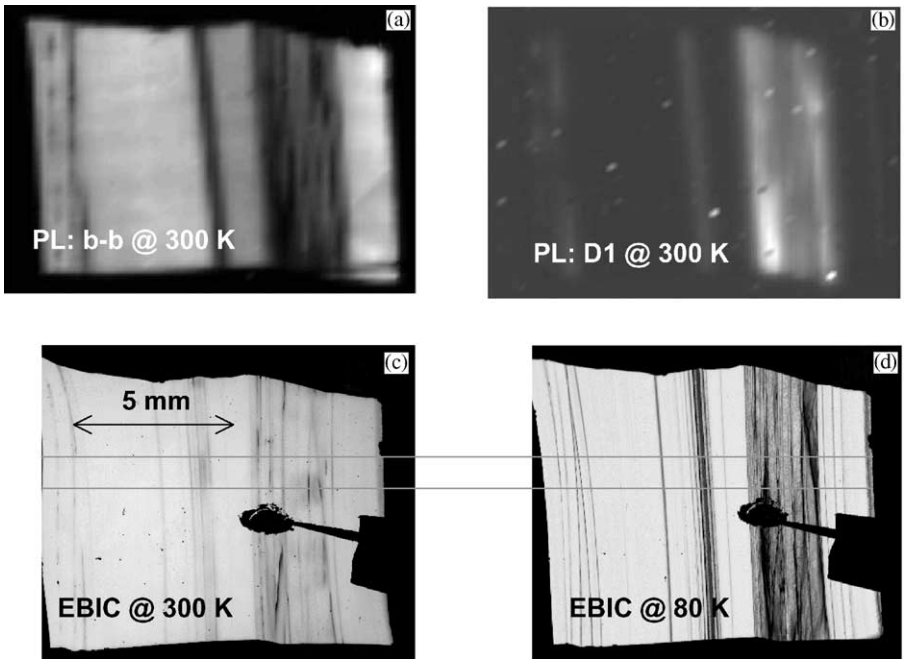

Fig. 4. Micrographs of room-temperature PL and EBIC taken from EFG-Si foils. The PL images present the intensity of band-to-band (a) and D1 luminescence (b) across the sample. (Note that the bright and dark spots in (b) are artifacts.) The EBIC micrographs are taken at 300 (c) and 80 K (d).

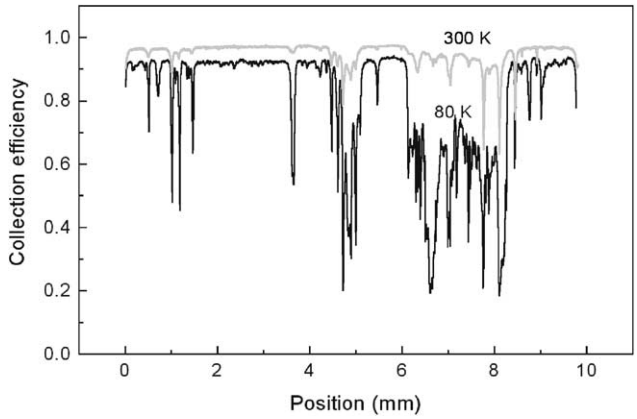

Fig. 5. Profiles of the EBIC collection efficiency taken at 80 (dark line) and 300 K (grey line) across the sample shown in Fig. 4. The reduction of the efficiency corresponds to defect-rich regions.

to be remarkably lower than that at 80 K. For some defects, the room-temperature activity even vanishes. These points are due to a relatively low contamination of dislocations in the order of 10 impurity atoms/μm of dislocation length. A more quantitative result would require $c(T)$ measurements on individual well-isolated

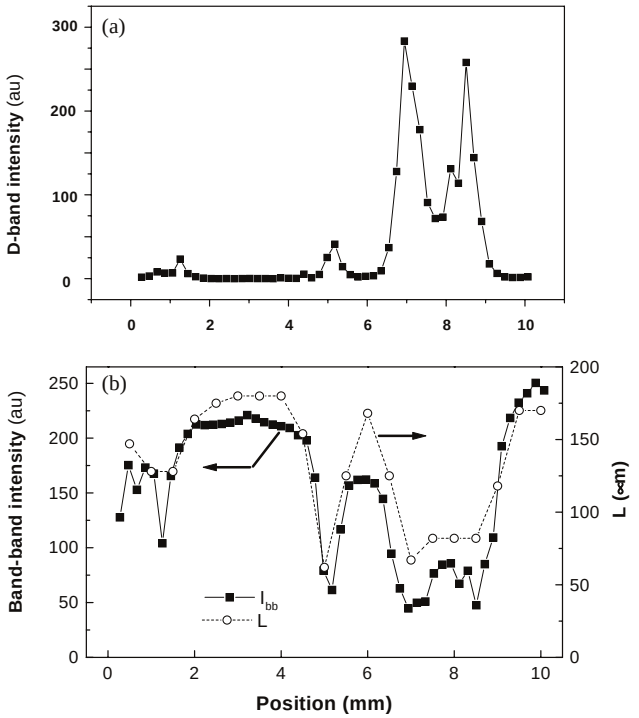

Fig. 6. Comparison of the profiles of D1-band luminescence (a), band-to-band luminescence and the minority-carrier diffusion length (b) measured at room temperature across the sample shown in Fig. 4.

dislocation with a well-defined geometry, which are not typical for the sample studied. Generally, the largely differing spatial resolution between EBIC and PL complicates the interpretation of experimental results. We feel that further upgrading in the spatial resolution of the luminescence apparatus could also help to extend the knowledge about the origin of defect luminescence.

Spectral response measurements were used to determine the spatial distribution of the minority-carrier diffusion length, L. Fig. 6 shows that the diffusion length profile correlates with the intensity of the band-to-band luminescence measured at room temperature but is in anti-correlation with the D1 luminescence. This is consistent with previously published results [8]. A smallest diffusion length of $\sim 70\,\mu m$ is found in defect areas. We conclude that the defects affecting the diffusion length are also responsible for the reduction of the band-to-band-luminescence and appearance of the D1 emission.

3. Conclusions

We demonstrated that scanning PL diagnostics at different spectral bands exhibits a large potential for non-contact and non-destructive characterisation of solar-grade

mc-Si. Both, band-to-band and D1 defect luminescence allow defect-imaging at room temperature. The intensity of the band-to-band luminescence correlates with the minority-carrier diffusion length. Concurrently, the D1 luminescence band appears in regions with relatively low diffusion length and its intensity is reversed to the band-band PL intensity. Dislocation-related effects in room-temperature PL were observed for both types 1 and 2 EBIC behaviour. It means that a relatively low contamination level of dislocations in the order of 10 impurity atoms/μm of the dislocation length produces D1 defect luminescence at room temperature and also degrades both the band-to-band luminescence and minority-carrier diffusion length. More details about the range of concentration of impurities at the dislocations and the kind of impurities under which the D1 defect luminescence can be observed are lacking so far. Also, the processes and the energy levels involved in the D1 defect luminescence are open questions.

Acknowledgements

The authors thank Dr. V. Higgs for performing SiPHER measurements on block-casting silicon. Part of this work has been supported by the German Bundesministerium für Wirtschaft under contract 29858H—KoSi project, and by the US National Renewable Energy Laboratory within the contract ACQ-9-29639-03.

References

[1] H.J. Möller, Solid State Phenom. 47–48 (1996) 127.
[2] M. Kittler, C. Ulhaq-Bouillet, V. Higgs, J. Appl. Phys. 78 (1995) 4573.
[3] M. Kittler, W. Seifert, Phys. Stat. Sol. A 150 (1995) 463.
[4] V. Kveder, M. Kittler, W. Schröter, Phys. Rev. B 63 (2001) 115208.
[5] N.A. Drozdov, A.A. Patrin, V.D. Tkatchev, Sov.-Phys. JETP Lett. 23 (1976) 597.
[6] M. Suezawa, K. Sumino, Phys. Stat. Sol. A 79 (1983) 173.
[7] R. Sauer, J. Weber, J. Stolz, E.R. Weber, K.H. Küsters, H. Alexander, Appl. Phys. A 1 (1985) 36.
[8] Y. Koshka, S. Ostapenko, I. Tarasov, S. McHugo, J.P. Kalejs, Appl. Phys. Lett. 74 (1999) 1555.
[9] S. Ostapenko, I. Tarasov, J.P. Kalejs, C. Hässler, E.-U. Reisner, Semicond. Sci. Technol. 15 (2000) 840.
[10] V.V. Kveder, E.A. Steinman, S.A. Shevchenko, H.G. Grimmeiss, Phys. Rev. B 51 (1995) 10520.
[11] E.A. Steinman, V.V. Kveder, V.I. Vdovin, H.G. Grimmeiss, Solid State Phenom. 69–70 (1999) 23.
[12] M. Suezawa, Y. Sasaki, K. Sumino, Phys. Stat. Sol. A 79 (1983) 173.
[13] V. Higgs, M. Goulding, A. Brinklow, P. Kightley, Appl. Phys. Lett. 60 (1992) 1369.
[14] V. Higgs, F. Chin, X. Wang, J. Mosalski, R. Beanland, J. Phys. Condens. Matter 12 (2000) 10105.
[15] V. Higgs, F. Chin, X. Wang, Solid State Phenom. 63–64 (1998) 421.
[16] A. Voigt, H.P. Strunk, Mater. Sci. Eng. B 24 (1994) 74.
[17] M. Kittler, W. Seifert, Phys. Stat. Sol. A 138 (1993) 687.